JOURNAL OF MATERIALS SCIENCE 19 (1984) 1314–1320

Kinetics of dissolution of silicon in CrO_3–HF–H_2O solutions

ROBERT B. HEIMANN
Atomic Energy of Canada Limited, Whiteshell Nuclear Research Establishment, Pinawa, Manitoba, R0E 1L0, Canada

Silicon wafers [*p*-type, B-doped, 10 Ω cm, dislocation density < 500 cm^{-2}, orientation (1 1 1)] have been dissolved in CrO_3–HF–H_2O solutions ("Sirtl etch") with molar concentration ratios $[Cr^{6+}]/[HF]$ between 0.03 and 0.72 at temperatures between 10 and 60° C. The dissolution kinetics suggests that silicon suboxides SiO_x $(0.67 < x < 1)$ are formed, and/or that the rate of diffusion of chromium is three times that of hydrofluoric acid.

1. Introduction

Etching of silicon wafers in Sirtl-type etchants [1] to determine the number and the type of dislocations present constitutes an important process step in semiconductor technology.

The dissolution reaction proceeds via oxidation of the silicon, the silicon oxide formed in turn being dissolved by the hydrofluoric acid. The total reaction can conveniently be described [2, 3] as a combined redox-reaction of areas of negative surplus charge (intrinsic *n*-type) and areas of positive (electron hole) surplus charge (intrinsic *p*-type):

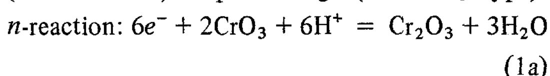

$$n\text{-reaction: } 6e^- + 2CrO_3 + 6H^+ = Cr_2O_3 + 3H_2O \qquad (1a)$$

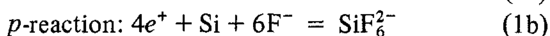

$$p\text{-reaction: } 4e^+ + Si + 6F^- = SiF_6^{2-} \qquad (1b)$$

Sirtl-type etchants have several advantages over the more commonly used etchants based on the system HNO_3–HF–H_2O (CH_3COOH): (i) the overall chemistry, though complex, does not involve induction reactions by transient reaction products of the nitric acid, (ii) the etchant exhibits pronounced selectivity for (1 1 1) and (1 1 0) orientations, (iii) samples etched in the HF–CrO_3 system at low hydrofluoric acid concentrations are less susceptible to staining because the effective concentration of the Cr^{6+} ions does not degrade as easily in air as does HNO_3 [4], and (iv) in the HF–CrO_3 system, the ability of the etchant to delineate lattice defects is less affected by small changes in the composition and the temperature of the etchant.

The present investigation deals with the kinetics of dissolution of silicon in Sirtl-type etches over a wide range of composition and temperature.

2. Experimental procedure*

The silicon wafers used were B-doped, *p*-type (10 Ω cm) and of (1 1 1) orientation with a dislocation density of < 500 cm^{-2}. Before etching, they were scribed with an alumina point, broken into squares approximately 10 mm by 10 mm, and cleaned according to a schedule recommended by Glendinning [5].

The etchants were always freshly prepared by mixing a stock solution of 50 g CrO_3 in 100 ml water with hydrofluoric acid (42%). The $[CrO_3]/[HF]$ molar concentration ratios were varied between 0.03 and 0.72. To slow down the reaction rates, the mixtures were diluted with double distilled water (1:1). For some experiments, Secco etch [6] was used.

Etching was carried out in polyethylene beakers surrounded by a heating jacket connected to a thermostat. The etching temperature was varied between 10 and 60° C and could be controlled to within ± 0.2° C at any given temperature.

The samples were suspended by a nylon thread,

*The experiments were conducted at the Institute for Materials Research, McMaster University, Hamilton, Ontario, L8S 4M1, Canada.

0022–2461/84 $03.00 + .12 © *1984 Chapman and Hall Ltd.*

and the etching solutions were agitated by a magnetic stirrer operating at $50\,r\,min^{-1}$. After the required etching time, the reaction was terminated by introducing a large volume of distilled water.

Weight losses were related to the original surface area of the samples and the dissolution rate expressed in $kg\,m^{-2}\,min^{-1}$.

The composition of the surface layers formed by etching was analysed qualitatively by scanning Auger electron spectroscopy.

3. Results

The temperature dependence of the rate of dissolution is shown in Fig. 1 for an etchant with a $[Cr^{6+}]/[HF]$ molar concentration ratio (ρ) of 0.48 and obeys an Arrhenius type law. Dissolution of silicon in etchants with other concentration ratios likewise yielded relationships of the type

$$\log V_s = -(A/T) \times 10^3 + B = -\frac{E}{2.303RT} \times 10^3 + \log A_0 \qquad (2)$$

where V_s is dissolution velocity, T is absolute temperature, R is the gas constant and is an empirical constant.

Table I gives the A and B parameters for all ρ-values investigated as well as the activation energies E.

Fig. 2 shows a log–log plot of the rate of dissolution as a function of the molar concentration ratio $\rho = [Cr^{6+}]/[HF]$ for 10 and 50° C. For small values of ρ, the rates are proportional to $\rho^{1/2}$; for higher values of ρ, the rates are proportional to ρ^{-p}. To the left of the maximum the concentration of chromium is small, and it is expected that the oxidation of silicon is the rate-determining step of the overall dissolution reaction [7]. To the right of the maximum surface-controlled dissolution of silicon oxide is probably the rate-determining step. These relations are also reflected by the morphology of etch pits on silicon surfaces with high dislocation densities. Fig. 3a shows crystallographically bounded pits on a silicon (1 1 1) surface etched for 30 min in original Sirtl [1] etch ($[CrO_3]/[HF] = 0.48$); Fig. 3b shows an

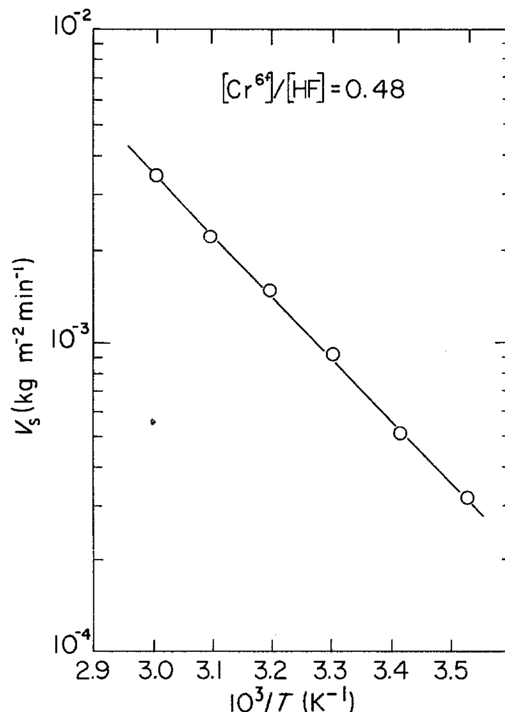

Figure 1 Arrhenius plot of the rate of dissolution of silicon (1 1 1) in Sirtl etch (molar concentration ratio $[Cr^{6+}]/[HF] = 0.48$) against the reciprocal of the absolute temperature.

TABLE I Slopes A and intercepts B of the function $\log V_s = -(A/T) \times 10^3 + B$, and calculated activation energies E of dissolution of Si(1 1 1) in etchants of Sirtl-type [1]. Etch time: 2 min.

$[Cr^{6+}]/[HF]$ ρ	$-A$ (K)	B	E (kJ mol^{-1})*	r†
0.03	2.025	4.043	38.8	− 0.995
0.06	1.921	3.866	36.8	− 0.993
0.08	1.687	3.126	32.3	− 0.999
0.12	1.798	3.419	34.4	− 0.998
0.16	1.797	3.363	34.4	− 0.986
0.24	1.892	3.601	36.2	− 0.994
0.36	1.961	3.579	37.5	− 0.991
0.48	1.995	3.532	38.2	− 0.998
0.72	2.040	3.667	39.0	− 0.996

*$E = 2.303 \times A \times R$ ($R = 8.313\,J\,K^{-1}\,mol^{-1}$).
†Correlation coefficient for linear regression.

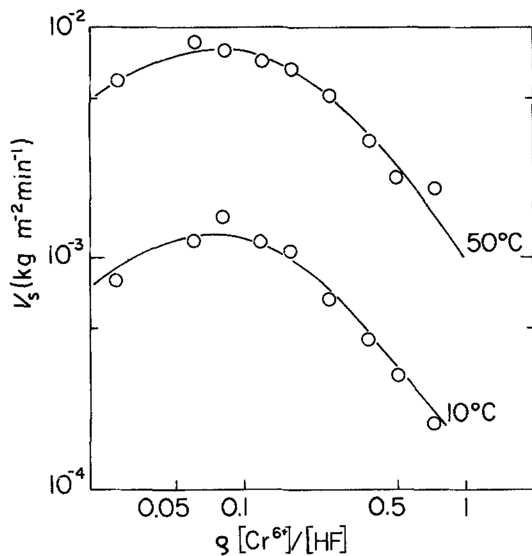

Figure 2 Rate of dissolution of silicon (111) as a function of the composition of the etchant.

identical specimen etched in Secco etch [6] with a $[CrO_3]/[HF]$ ratio of 6×10^{-3} [8]. The circular shape of the pits in Fig. 3b suggests diffusion of the oxidizing chromate ion towards the reacting interface. Moreover, for the Secco etch, the etch rate depends stronly on stirring rate, which is consistent with a diffusion-controlled mechanism. Hence, it is possible to assign two general equations to both branches of the curve of Fig. 2:

$$V_s(\mathrm{ox}) = k_1 \rho^{1/2} \qquad \text{for } \rho < \rho(\max) \quad (3a)$$

$$V_s(\mathrm{diss}) = k_2 \rho^{-p} \qquad \text{for } \rho > \rho(\max). \quad (3b)$$

The overall rate of dissolution might be tentatively described by linear combination of V_s (ox) and V_s (diss), and the rate constants k_i depend on the temperature as

$$k_i = K_i \exp(-\beta_i/T). \quad (4)$$

Curve fitting of the data points yields

$$V_s = \frac{K_1 \times K_2 \exp[-(\beta_1 + \beta_2)/T] \times \rho^{1/2}}{K_2 \exp[-\beta_2/T] + K_3 \exp[-\beta_1/T] \times \rho^{p+1/2}}$$

$$(283 < T < 333\,\mathrm{K}) \quad (5)$$

with $K_1 = 2.026 \times 10^4\,\mathrm{kg\,m^{-2}\,min^{-1}}$, $K_2 = 7.178 \times 10^3\,\mathrm{kg\,m^{-2}\,min^{-1}}$, $K_3 = 1.733 \times 10^5\,\mathrm{kg\,m^{-2}\,min^{-1}}$, $\beta_1 = 4248\,\mathrm{K}$, $\beta_2 = 4406\,\mathrm{K}$, and $p = 4/3$. These curves are shown in Fig. 2 as solid lines. To obtain the ρ value at the maximum rate of dissolution, the first derivative of Equation 5 is equated to zero ($dV_s/d\rho = 0$). For the two temperatures shown in Fig. 2, the ρ(max) values are 0.076 for 10° C and 0.079 for 50° C, respectively.

The apparent activation energies E are plotted against the molar concentration ratio ρ in Fig. 4.

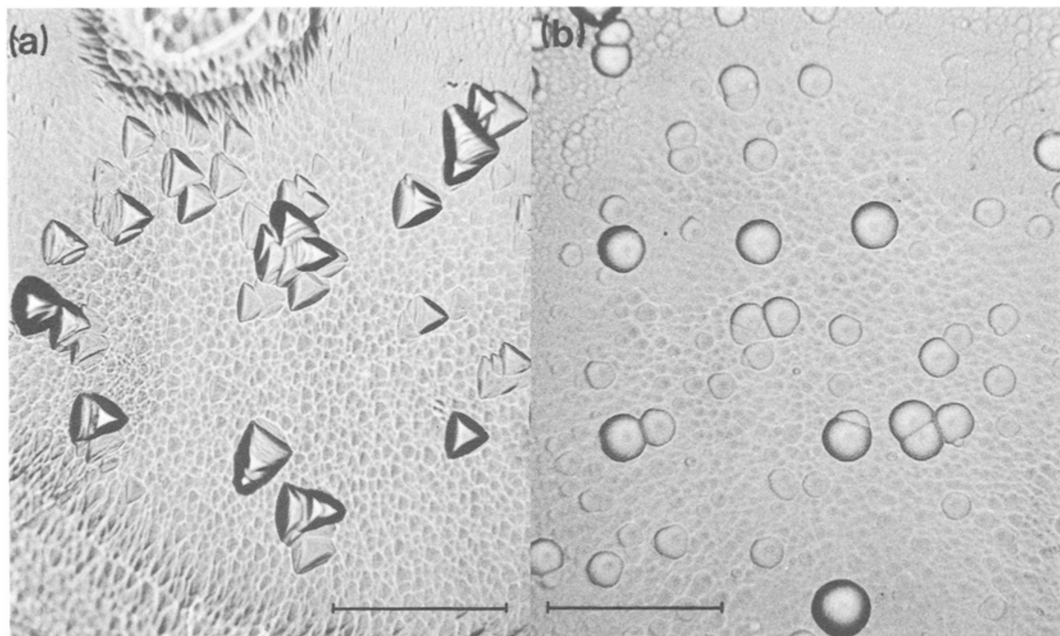

Figure 3 Silicon (111), dislocation density $1.5 \times 10^5\,\mathrm{cm^{-2}}$, etched in (a) Sirtl etch for 30 min, (b) Secco etch for 30 min. Bar corresponds to 50 μm (according to [8]).

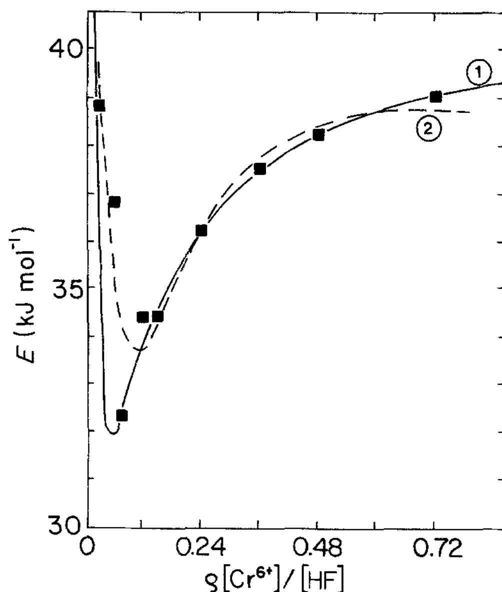

Figure 4 Activation energy of dissolution of silicon (111) as a function of the composition of the etchant. The solid curve (1) corresponds to a Mie-type function, the dashed curve (2) is of Morse-type.

The measured points were fitted to functions of the type

$$E = E_0/n - am\rho^{-n} + bn\rho^{-m} \quad (6)$$

with $E_0 = 40.96\,\mathrm{kJ\,mol^{-1}}$, $a = 5055.5\,\mathrm{kJ\,mol^{-1}}$, $b = 5054\,\mathrm{kJ\,mol^{-1}}$, $n = 1$, $m = 1.0001$, and

$$E = E_0 + c\{\exp[-2\alpha(\rho - \rho_0)] - 2\exp[-\alpha(\rho - \rho_0)]\} \quad (7)$$

with $E_0 = 38.79\ \mathrm{kJ\,mol^{-1}}$, $c = 5.06\ \mathrm{kJ\,mol^{-1}}$, $\alpha = 8.786$, $\rho_0 = 0.11$.

Equation 6 is a mathematical analogy to an energy potential Mie function, whereas Equation 7 resembles a Morse function. The former yields a better fit for values $\rho > \rho(\mathrm{min})$ (oxide dissolution reaction), whereas the latter yields a better fit for values $\rho < \rho(\mathrm{min})$ (oxidation reaction). The Morse-type function, however, fails to reproduce the experimentally obtained minimum activation energy for $\rho = 0.08$.

4. Discussion

Dissolution of semiconductor single crystals in a redox etchant frequently yields curves of the type depicted in Fig. 2. Similar curves were reported by Camp [9] for dissolution of germanium in H_2O_2/HF, for silicon dissolved in HNO_3/HF by Robbins and Schwartz [7] and Klein and D'Stefan [3], and for gallium arsenide dissolved in CrO_3/HF by Heimann [10].

Turner [2] pointed out that for dissolution of silicon in HNO_3/HF solutions the maximum rate of dissolution is expected for $[HNO_3]/[HF]$ ratios of 0.22, corresponding to the stoichiometry of the reaction

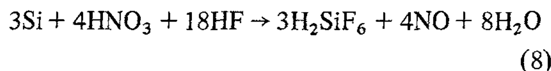

$$3Si + 4HNO_3 + 18HF \rightarrow 3H_2SiF_6 + 4NO + 8H_2O \quad (8)$$

if both the oxidation step of silicon and the molecular reaction of silicon oxide to form H_2SiF_6 are assumed to be instantaneous [3].

The redox reaction of Equation 8 involves a three-electron change. Likewise, the dissolution reaction for silicon in the CrO_3–HF requires the transfer of three charges according to

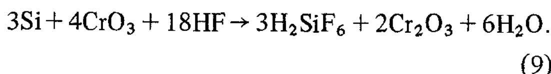

$$3Si + 4CrO_3 + 18HF \rightarrow 3H_2SiF_6 + 2Cr_2O_3 + 6H_2O. \quad (9)$$

The experimental results indicate that the maximum rate of dissolution occurs at a molar concentration ratio $\rho \simeq 0.1$ which is significantly lower than the ratio of 0.22 expected by analogy with Equation 8.

To explain this discrepancy four different mechanisms are envisaged:

(i) Formation of intermediate reaction products;

(ii) Differences in the apparent diffusion coefficients of hydrofluoric acid and the hydrated chromium(VI) ion complex;

(iii) Change of the mass action constants for the dissociation and association reactions of hydrofluoric acid with concentration; and

(iv) Incomplete oxidation of silicon by three-electron transfer at low chromium (VI) ion concentrations.

4.1. Formation of intermediate reaction products

The results of Schwartz and Robbins [11] indicate that the HNO_3/HF molar ratio corresponding to the maximum rate of dissolution of silicon is lower by a factor of 1.5 than the stoichiometric ratio of 0.22. They attempted to resolve the apparent discrepancy by taking into account a dissolution mechanism involving reactions by autocatalytically-formed HNO_2. Thus, the stoichiometry of the reaction is not determined by the actual surface reaction, but by reactions within the boundary layer between silicon and the etchant, and in the bulk solution.

In the present case, likely intermediate reaction products would be chromylfluoride or tetrafluorodisiloxane [12]. The mass action constants of the hydrolysis reaction of these compounds, however, are so large that no appreciable concentrations of intermediate species can be built up in the interface layer.

4.2. Differences in apparent diffusion coefficients

The stoichiometric ratio of oxidant and solvent is only important in influencing the maximum rate of reaction if the diffusion coefficients of both species, and their temperature dependencies, are comparable and if the reactions are essentially instantaneous. Hence, the deviation of the experimentally observed molar concentration ratio from the stoichiometric ratio could be explained assuming that the diffusion coefficient of the hydrated chromium (VI) ion complex is approximately 3 times that of the hydrofluoric acid over the temperature range 10 to 60° C. This view is supported by the empirical finding of Sirtl and Adler [1] that the optimum concentration ratio for development of etch pits on silicon surfaces is H_2O/HF (water-free)/CrO_3 = 1:0.4:0.2 by weight. This weight ratio translates into a molar concentration ratio $[CrO_3]/[HF] = 0.1$, which is reasonably close to the results described in this work.

Even stronger corroboration of the assumption that the diffusion coefficient of chromium (VI) ions towards the reaction interface is much larger than that of hydrofluoric acid is given in a recent paper by Lue and Meyer [13]. They obtained Rutherford back-scattering spectra from silicon etched in Sirtl etch which suggested diffusion of chromium atoms deep into the silicon surface under the driving force of a proposed local temperature as high as 250° C. This local temperature increase was related to heat release by exothermal etching of SiO_2 by HF which in turn was used for the oxidation of silicon by CrO_3 and the accelerated diffusion of chromium.

4.3. Change of mass action constants

Several studies of the dissolution of silicon dioxide in fluoride-based etchants yielded activation energy values in the range of those observed during the present investigation [14–16]. Most notably, Judge [14] determined the rate of dissolution of SiO_2 in dilute acidic fluoride solutions to be:

$$R\,(\mathrm{nm\,sec^{-1}}) = 5.0\times10^{6}\,[HF_2^-]\exp(-\Delta E_1/RT) + 2.2\times10^{5}\,[HF]\exp(-\Delta E_2/RT) + C(T) \quad (10)$$

where $\Delta E_1 = 38\,\mathrm{kJ\,mol^{-1}}$, $\Delta E_2 = 33.8\,\mathrm{kJ\,mol^{-1}}$, $C(T) = 0.025\,(T-292)$.

Evidently, the concentration of the free fluoride ion $[F^-]$ does not play an important role. The activation energy ΔE_1 refers to the dissolution reaction governed by attack of $[HF_2^-]$, the lower activation energy ΔE_2 is related to the [HF] reaction. Hence, the dependence of the activation energy of dissolution of silicon in CrO_3/HF solutions as shown in Fig. 4 reflects the decrease of the $[HF_2^-]$ concentration with decreasing total fluoride concentration, i.e. with decreasing [HF]. In highly concentrated hydrofluoric acid corresponding to small ρ-values the dissociation constant K_1 is small:

$$K_1 = \frac{[H^+][F^-]}{[HF]} = 1.3\times10^{-3} \quad \text{at } 25^\circ\text{C [17].}$$

Thus, $[F^-]$ required for the reaction

$$F^- + HF \rightleftarrows HF_2^-$$

is small, and the overall dissolution kinetics are governed by the abundant [HF] leading to activation energy values around 33 kJ mol^{-1} as required according to Judge [14]. More concentrated hydrofluoric acid solutions produce HF_2^-, according to

$$K_2 = \frac{[HF][F^-]}{[HF_2^-]} = 0.104 \quad \text{at } 25^\circ\text{C [17]}$$

and is reflected by an increase in the apparent activation energy to values around 38 kJ mol^{-1}. Moreover, high activation energies of 43 kJ mol^{-1} for the $[HF_2^-]$ reaction were given by Kozhevnikov *et al.* [15]. The etch rates varied as

$$R \propto [HF_2^-]^{1.35}.$$

The exponent is close to the value of $p = 4/3$ found for the dissolution reaction according to Equation 3b, suggesting a diffusion-controlled mechanism for highly concentrated hydrofluoric acid solutions.

4.4. Incomplete oxidation of silicon

Redox etching solutions for silicon involving transfer of only three or fewer charges generally give rise to formation of so-called chemical stain [4, 7,

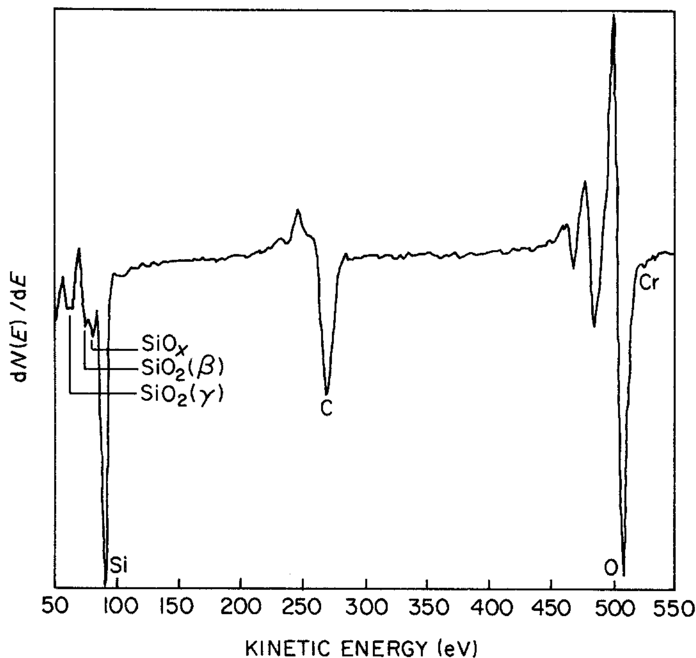

Figure 5 Derivative Auger electron spectrum $dN(E)/dE$ of a silicon (111) surface etched for 15 min in Secco etch (2 parts HF (49%) + 1 part 0.15M $K_2Cr_2O_7$; $[Cr^{6+}]/[HF] = 6 \times 10^{-3}$].

11, 18]. Its origin is the incomplete oxidation of silicon forming silicon suboxides SiO_x ($x < 2$). In CrO_3/HF solutions with low concentrations of chromium(VI) ions, the oxidation reaction leads to a fast depletion of the oxidizing agent in the vicinity of the silicon/solution interface owing to the high oxidation rate of the highly doped silicon surface [4]. High doping levels shift the Fermi energy level towards the valence band in *p*-type silicon, and in turn provide vacancies in the substrate. These vacancies lead to enhanced oxidation [19]. Hence, overall reaction equations can be formulated such as

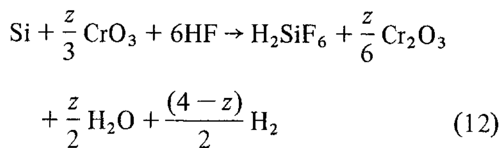

$$\mathrm{Si} + \frac{z}{3}\mathrm{CrO_3} + 6\mathrm{HF} \rightarrow \mathrm{H_2SiF_6} + \frac{z}{6}\mathrm{Cr_2O_3} + \frac{z}{2}\mathrm{H_2O} + \frac{(4-z)}{2}\mathrm{H_2} \qquad (12)$$

for $z \leqslant 4$, where z is the number of electron holes required to oxidize the elemental silicon. The number of holes, z, decreases in the order 4, 3, 2, 3/2 for the silicon oxides SiO_2, Si_2O_3, SiO, and Si_3O_2, respectively.

Likewise, the $[CrO_3]/[HF]$ molar concentration ratio, ρ, decreases for $z = 4, 3, 2, 3/2$ in the order $\rho = 0.22, 0.16, 0.11, 0.083$.

Fig. 5 shows the first derivative high resolution Auger spectrum of a silicon surface etched for 15 min in Secco etch. Towards the low energy side of the $L_{2,3}VV$ peak of elemental silicon at 91 eV are at least three aditional peaks at 81.5, 75, and 62.5 eV. These peaks can be assigned to $SiO_x (x < 2)$, $SiO_2(\beta)$, and $SiO_2(\gamma)$ [20]. The strong carbon *KLL* peak at 270 eV shows features typical of graphitic carbon [21, 22]. There is a faint peak at 525 eV attributable to chromium ($6 \pm 3\%$ of a monolayer). Sputtering with Xenon gas at 5 keV for only 15 sec removes chromium completely, decreases the $SiO_2(\gamma)$ and SiO_x signals appreciably, and also reduces the intensity of the oxygen and carbon peaks. At the high energy side of the main silicon peak, a new peak at 107 eV appears which is either related to a plasmon gain mechanism [23], or has its origin in a double ionization of the ground state of silicon [24]. From the ion sputter rate, the thickness of the oxide layer is calculated to be approximately 15 nm. Thus, even in the presence of very small amounts of chromium(VI) ions ($\rho = 6 \times 10^{-3}$), a relatively thick oxide layer is retained after etching, showing that the rate of the silicon suboxide formation is greater than the rate of its dissolution [4].

5. Conclusions

Dissolution of *p*-type silicon in CrO_3–HF–H_2O etches according to Sirtl [1] yields kinetic results implying a two-step mechanism. In the first step silicon is oxidized by the Cr^{6+} ion. The second step consists of dissolution of the silicon oxide in hydrofluoric acid. The maximum rate of dissolution has been observed at a molar concen-

tration ratio $[Cr^{6+}]/[HF]$ $\rho = 0.08$ (Fig. 2). The minimum activation energy is found for $\rho = 0.074$ (Mie-function) and $\rho = 0.11$ (Morse-function), respectively (Fig. 3). These values are at variance with the stoichiometric ratio $\rho = 0.22$. It is therefore suggested that the oxidation product is a silicon suboxide SiO_x with $0.67 < x < 1$. Silicon suboxides are responsible for chemical staining of silicon generally observed in etchants with transfer of three or fewer charges. An alternative explanation for the deviation of the molar concentration ratio for maximum dissolution rate from the stoichiometric ratio is based on the assumption that the rate of diffusion of chromium is approximately three times that of hydrofluoric acid.

Acknowledgements

I am indebted to Mr Pierre Zaya, Alcan, Kingston, Ontario and to Mr Andrew White, AECL, Pinawa, Manitoba for computing the curve fitting routines of Equations 5, 6 and 7. Dr M. J. Graham, National Research Council, Ottawa kindly provided the Auger analyses. The help and financial assistance of Professor M. Brian Ives, McMaster University, Hamilton is gratefully acknowledged. Parts of this work were supported by a research grant by Deutsche Forschungsgemeinschaft.

References

1. E. SIRTL and A. ADLER, *Z. Metallkde.* 52 (1961) 529.
2. D. R. TURNER, *J. Electrochem. Soc.* 107 (1960) 810.
3. D. L. KLEIN and D. J. D'STEFAN, *ibid.* 109 (1962) 37.
4. D. G. SCHIMMEL and M. J. ELKIND, *ibid.* 125 (1978) 152.
5. W. B. GLENDINNING, W. B. PHARO and D. W. YARBROUGH, Research and Development Technical Report ECOM-4061, US Army Electronics Command, Fort Monmouth, NJ (1972).
6. F. SECCO D'ARAGONA, *J. Electrochem. Soc.* 119 (1972) 948.
7. H. ROBBINS and B. SCHWARTZ, *ibid.* 106 (1959) 505.
8. R. B. HEIMANN, in "Crystals, Growth, Properties, and Applications", Vol. 8, edited by J. Grabmaier (Springer, Berlin, Heidelberg, New York, 1982) p. 207.
9. P. R. CAMP, *J. Electrochem. Soc.* 102 (1955) 586.
10. R. B. HEIMANN, *Z. Phys. Chem., N.F.* 104 (1977) 11.
11. B. SCHWARTZ and H. ROBBINS, *J. Electrochem. Soc.* 108 (1961) 365.
12. J. L. MARGRAVE, K. G. SHARP and P. W. WILSON, *J. Amer. Chem. Soc.* 92 (1970) 1530.
13. J. T. LUE and O. MEYER, *J. Appl. Phys.* 54 (1983) 1148.
14. J. S. JUDGE, *J. Electrochem. Soc.* 118 (1971) 1772.
15. L. D. KOZHEVNIKOV, N. A. VELESHKO, S. N. SPIRIN and E. G. RAKOV, *Russ. J. Inorg. Chem.* 22 (1977) 1850.
16. J. K. VONDELING, *J. Mater. Sci.* 18 (1983) 304.
17. R. E. MESMER and G. F. BAES, *Inorg. Chem.* 8 (1969) 618.
18. R. B. HEIMANN, M. B. IVES and N. S. McINTYRE, *Thin Solid Films* (in press).
19. C. P. HO and J. S. PLUMMER, *J. Electrochem. Soc.* 126 (1979) 1516.
20. B. LANG, P. SCHOLLER and B. CARRIERE, *Surface Sci.* 99, (1980) 103.
21. C. C. CHANG, *ibid.* 23(1970) 283.
22. E. KNY, *J. Vac. Sci. Technol.* 17 (1980) 658.
23. M. F. CHUNG and L. H. JENKINS, *Surface Sci.* 26 (1971) 649.
24. S. THOMAS, *J. Appl. Phys.* 45 (1974) 161.

Received 17 June
and accepted 28 July 1983